

Robotics Modeling
**Modeling and control of underwater vehicle:
Sparus**

Students:
Anastasia Frolova
Shahid Ahamed Hasib

Course Title: Underwater Robotics, Modeling and Control

Instructor:
Dr. Mathieu RICHIER

Submitted on January 10, 2025

1 Results

Work to do 1:

With the figure 2, compute all the dimension of the different bodies

The overall dimensions of the Sparus AUV have been illustrated in Figure 1.

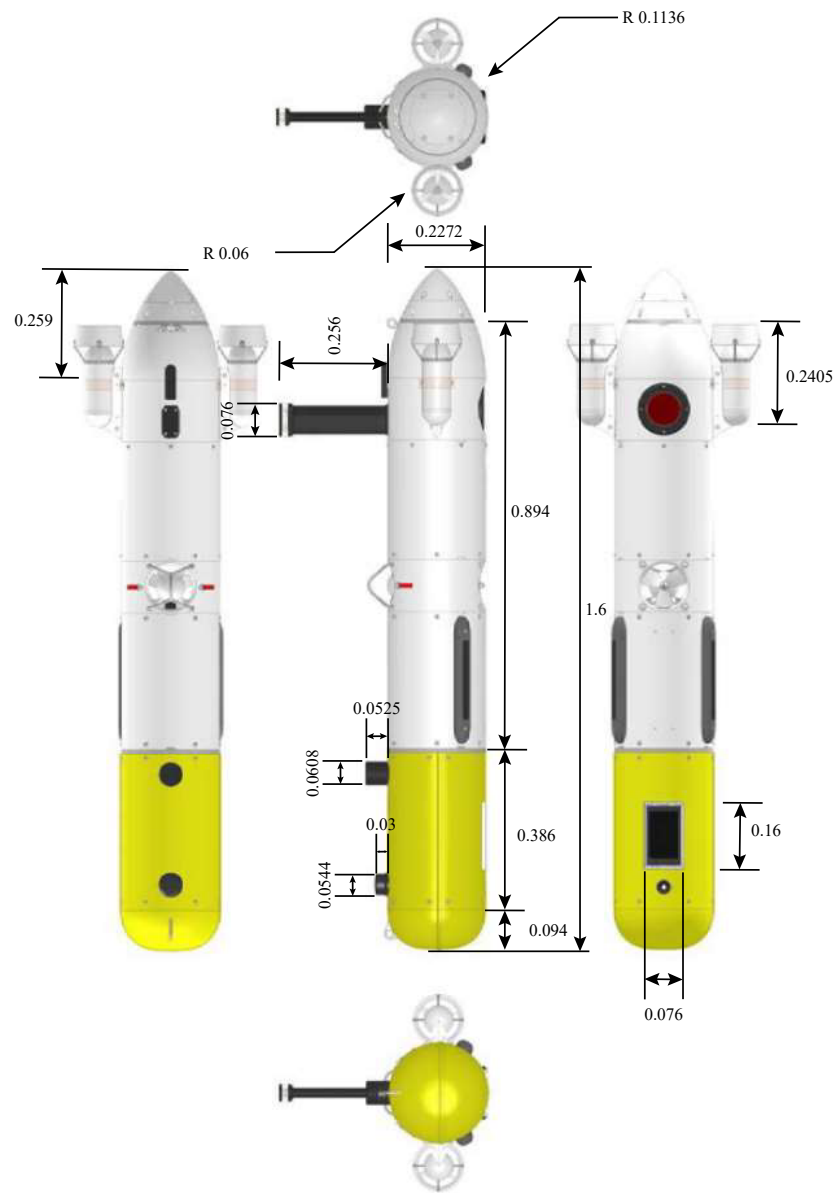


Figure 1: Dimensions of Sparus AUV

Work to do 2:

Considering the given global real mass matrix explains all the terms: from which part the various terms in the matrix originate.

$$M_{\text{CO}}^{\text{RB}} = \begin{bmatrix} 52 & 0 & 0 & 0 & -0.1 & 0 \\ 0 & 52 & 0 & 0.1 & 0 & -1.3 \\ 0 & 0 & 52 & 0 & 1.3 & 0 \\ 0 & 0.1 & 0 & 0.5 & 0 & 0 \\ -0.1 & 0 & 1.3 & 0 & 9.4 & 0 \\ 0 & -1.3 & 0 & 0 & 0 & 9.5 \end{bmatrix}$$

It is 6×6 matrix, which is combined of 4 matrices with dimensions 3×3

$$\begin{aligned} M_{\text{RB}}^{\text{CO}} &= \begin{bmatrix} mI_{3x3} & -mS(r_g^b) \\ mS(r_g^b) & I_0 \end{bmatrix} \\ &= \begin{bmatrix} m & 0 & 0 & 0 & mz_g & -my_g \\ 0 & m & 0 & -mz_g & 0 & mx_g \\ 0 & 0 & m & 0 & -mx_g & 0 \\ 0 & -mz_g & 0 & I_x & -I_{xy} & -I_{xz} \\ mz_g & 0 & -mx_g & -I_{yx} & I_y & -I_{yz} \\ -my_g & mx_g & 0 & -I_{zx} & -I_{zy} & I_z \end{bmatrix} \end{aligned}$$

where

m is mass of the body, measured in kg ,

I_x , I_y and I_z are moments of inertia of the body, measured in $\frac{\text{kg}}{\text{m}^2}$,

$S(r)$ is cross-product matrix (or Skew-symmetric matrix).

Interpretation of the matrix can be done the following way:

1. Matrix $mS(r_g^b)$ shows how applied inertia (linear movement) effects angular rotations
 - (a) movement along x-axis (surge) gives a slight anti-clockwise rotation over y-axis (pitch = 0.1) that is caused by the antenna on the front part of Sparus;
 - (b) movement along y-axis (sway) gives a slight clockwise rotation over x-axis (roll = -0.1) that is caused by antenna on the front part, and a bigger anti-clockwise rotation over z-axis (yaw = 1.3) that is caused by antenna and the thrusters on the front part;
 - (c) movement along z-axis (heave) gives a slight clockwise rotation over y-axis (pitch = -1.3) that is caused by heavier front part.
2. Matrix I_0 shows how mass mass is distributed relative to x, y and z rotation axes
 - (a) Rotations along y and z axes (pitch and yaw) give almost identical result because z and y radius of Sparus are the same;
 - (b) The only difference is due to the fact that 2 thrusters with bigger dimensions influence on y-axis rotation (9.4), while the antenna with smaller dimension influence on z-axis rotation (9.5);
 - (c) Rotation along x (roll) is way smaller due to way smaller radius.
3. Matrix mI_{3x3} is diagonal matrix with constant mass of the body equals to 52 kg.

Work to do 3:

Compute each added mass matrix at the buoyancy center of the sparus. Excepted the main body, the CG and CB of the other bodies are at the same point.

Four added mass matrices must be computed: the antenna, both thrusters, and the main body. A combination of the Slender Body Theory and Lamb's k-factors is used.

	1	2	3	4	5	6
1						
2		$m_{22} = \int_L a_{22} dx$				$m_{26} = \int_L x a_{22} dx$
3			$m_{33} = \int_L a_{33} dx$		$m_{35} = -\int_L x a_{33} dx$	
4				$m_{44} = \int_L a_{44} dx$		
5			$m_{53} = -\int_L x a_{33} dx$		$m_{55} = \int_L x^2 a_{33} dx$	
6		$m_{62} = \int_L x a_{22} dx$				$m_{66} = \int_L x^2 a_{22} dx$

Table 1: Added Mass - Slender Body Theory

$$a_{nn} = \int_0^L \pi \rho C_A r^2 dx$$

$$m_{nn} = \int_L x^2 a_{nn} dx$$

As we assumed Sparus' parts' shapes to be cylindrical, C_A terms are equal to 1 in all formulas. For calculating Lamb's k-factors following equations are used:

$$m_{df} = \frac{4}{3} p \pi a b^2$$

$$e = \sqrt{1 - \frac{b^2}{a^2}}$$

$$\alpha_0 = 2 \frac{1 - e^2}{e^3} \left(\frac{1}{2} \ln \left[\frac{1+e}{1-e} \right] - e \right)$$

$$k_1 = \frac{\alpha_0}{2 - \alpha_0}$$

$$m_{11} = k_1 * m_{df}$$

For translation body from point to point, for example from CG to CB, following formulas are used:

$$M_A^{CG} = H^T(\vec{AB}) M_B^{CG} H(\vec{AB})$$

where

$$H(\vec{AB}) = \begin{bmatrix} I_{3x3} & S^T(\vec{AB}) \\ O_{3x3} & I_{3x3} \end{bmatrix}$$

$$S(\lambda) = \begin{bmatrix} 0 & -\lambda_3 & \lambda_2 \\ \lambda_3 & 0 & -\lambda_1 \\ -\lambda_2 & \lambda_1 & 0 \end{bmatrix},$$

$$\lambda = \begin{bmatrix} \lambda_1 \\ \lambda_2 \\ \lambda_3 \end{bmatrix} \text{ is a translational vector}$$

For **antenna** the characteristic length of the body in the longitudinal direction is considerably larger than the body's characteristic length in the other two directions: the slenderness ratio $\frac{L}{d} \geq 10$ (min 5).

$$\frac{0.256}{0.0256} \geq 10$$

Therefore slender body theory can be used for the antenna. The antenna is considered symmetrical in all three planes (XY, YZ, XZ), resulting in only six diagonal coefficients to estimate. However, the antenna is a slender body along the z-axis rather than the x-axis, as shown in Table 1. This implies that certain coefficients, such as m_{33} (movement along z-axis) are excessive and should be neglected. Also it means that there is coefficient m_{11} that are absent in slender body theory so it should be calculated using Lamb's k-factors.

So the added mass matrix calculated version is shown below:

$$M_{antenna} = \begin{bmatrix} 0.0804 & 0 & 0 & 0 & 0 & 0 \\ 0 & 1.1892 & 0 & 0 & 0 & 0 \\ 0 & 0 & 0 & 0 & 0 & 0 \\ 0 & 0 & 0 & 0.0057 & 0 & 0 \\ 0 & 0 & 0 & 0 & 0.0056 & 0 \\ 0 & 0 & 0 & 0 & 0 & 0.0260 \end{bmatrix}$$

Then, we need to translate the antenna matrix to the gravity center of the entire body using the translational vector $[-0.438; 0; -0.225]$. Therefore, the translated antenna added mass matrix is shown below:

$$M_{antennatrans}^{CG} = \begin{bmatrix} 0.0804 & 0 & 0 & 0 & -0.0181 & 0 \\ 0 & 1.1892 & 0 & 0.2675 & 0 & -0.5209 \\ 0 & 0 & 0 & 0 & 0 & 0 \\ 0 & 0.2675 & 0 & 0.0659 & 0 & -0.1172 \\ -0.0181 & 0 & 0 & 0 & 0.0097 & 0 \\ 0 & -0.5209 & 0 & -0.1172 & 0 & 0.2541 \end{bmatrix}$$

It is also possible to neglect terms that are less than 0.1 due to their small impact on the body. As a result, the final translated antenna added mass matrix is shown below:

$$M_{finalantennatrans}^{CG} = \begin{bmatrix} 0 & 0 & 0 & 0 & 0 & 0 \\ 0 & 1.19 & 0 & 0.27 & 0 & -0.52 \\ 0 & 0 & 0 & 0 & 0 & 0 \\ 0 & 0.27 & 0 & 0 & 0 & -0.12 \\ 0 & 0 & 0 & 0 & 0 & 0 \\ 0 & -0.52 & 0 & -0.12 & 0 & 0.25 \end{bmatrix}$$

For the **thrusters**, a combination of two theories will be used to calculate the terms. For the added mass coefficient m_{11} Lamb's k-factor is applied, while m_{22} and m_{66} are set to 0. Movement along the y-axis (m_{22}) and rotation around the z-axis (m_{66}) will not affect the added mass of the whole body because the thrusters are "hidden" inside the main body. The thrusters are modeled as cylinders with an average diameter of 0.1 m.

$$M_{thruster} = \begin{bmatrix} 0.2073 & 0 & 0 & 0 & 0 & 0 \\ 0 & 0 & 0 & 0 & 0 & 0 \\ 0 & 0 & 2.6275 & 0 & 0 & 0 \\ 0 & 0 & 0 & 0.0032 & 0 & 0 \\ 0 & 0 & 0 & 0 & 0.0507 & 0 \\ 0 & 0 & 0 & 0 & 0 & 0 \end{bmatrix}$$

After using translational vectors $[-0.59; 0.17; 0]$ and $[-0.59; -0.17; 0]$ the translated thrusters (left and right) added mass matrix is shown below:

$$M_{\text{thrusterleft}}^{\text{CG}} = \begin{bmatrix} 0.2073 & 0 & 0 & 0 & 0 & 0.0352 \\ 0 & 0 & 0 & 0 & 0 & 0 \\ 0 & 0 & 2.6275 & -0.4467 & 1.5503 & 0 \\ 0 & 0 & -0.4467 & 0.0792 & -0.2635 & 0 \\ 0 & 0 & 1.5503 & -0.2635 & 0.9653 & 0 \\ 0.0352 & 0 & 0 & 0 & 0 & 0.0060 \end{bmatrix}$$

$$M_{\text{thrusterright}}^{\text{CG}} = \begin{bmatrix} 0.2073 & 0 & 0 & 0 & 0 & -0.0352 \\ 0 & 0 & 0 & 0 & 0 & 0 \\ 0 & 0 & 2.6275 & 0.4467 & 1.5503 & 0 \\ 0 & 0 & 0.4467 & 0.0792 & 0.2635 & 0 \\ 0 & 0 & 1.5503 & 0.2635 & 0.9653 & 0 \\ -0.0352 & 0 & 0 & 0 & 0 & 0.0060 \end{bmatrix}$$

Neglecting terms less than 0.1 due to their minimal impact, the final translated added mass matrices for the left and right thrusters are as follows:

$$M_{\text{finalthrusterleft}}^{\text{CG}} = \begin{bmatrix} 0.2 & 0 & 0 & 0 & 0 & 0 \\ 0 & 0 & 0 & 0 & 0 & 0 \\ 0 & 0 & 2.63 & -0.45 & 1.55 & 0 \\ 0 & 0 & -0.45 & 0 & -0.26 & 0 \\ 0 & 0 & 1.55 & -0.26 & 0.96 & 0 \\ 0 & 0 & 0 & 0 & 0 & 0 \end{bmatrix}$$

$$M_{\text{finalthrusterright}}^{\text{CG}} = \begin{bmatrix} 0.2 & 0 & 0 & 0 & 0 & 0 \\ 0 & 0 & 0 & 0 & 0 & 0 \\ 0 & 0 & 2.63 & 0.45 & 1.55 & 0 \\ 0 & 0 & 0.45 & 0 & 0.26 & 0 \\ 0 & 0 & 1.55 & 0.26 & 0.96 & 0 \\ 0 & 0 & 0 & 0 & 0 & 0 \end{bmatrix}$$

Main body has torpedo shape, which means that $m_{11}, m_{22}, m_{33}, m_{55}, m_{66}, m_{53}, m_{35}, m_{62}, m_{26}$ coefficients have to be estimated with $m_{35} = m_{26}, m_{22} = m_{33}, m_{55} = m_{66}$ due to axis-symmetry with respect to x-axis. Coefficient m_{44} is not considered here and equals to 0 because rotation around x-axis will not affect water mass movement due to Sparus cylindrical shape. Coefficient m_{11} is calculated through Lamb's k-factor, the rest are calculated using Slender Body theory.

To calculate the terms for the main body, it is divided into three parts: a right circular cylinder with a length of 1.2515 m, and two hemispheres located at the front and back of Sparus with lengths of 0.246 m and 0.1025 m, respectively. The radius remains constant at 0.115 m for all parts. Each part is integrated separately, and the results are summed to obtain the matrix terms shown below.

$$M_{\text{body}}^{\text{CG}} = \begin{bmatrix} 1.6038 & 0 & 0 & 0 & 0 & 0 \\ 0 & 57.3280 & 0 & 0 & 0 & 10.9245 \\ 0 & 0 & 57.3280 & 0 & -10.9245 & 0 \\ 0 & 0 & 0 & 0 & 0 & 0 \\ 0 & 0 & -10.9245 & 0 & 15.0487 & 0 \\ 0 & 10.9245 & 0 & 0 & 0 & 15.0487 \end{bmatrix}$$

As the main body added mass matrix already is calculated in center of gravity we do not need to translate the matrix.

Now we can calculate added mass matrix for **USBL** using both theories as before:

$$M_{usbl} = \begin{bmatrix} 0.0605 & 0 & 0 & 0 & 0 & 0 \\ 0 & 0.0320 & 0 & 0 & 0 & 0 \\ 0 & 0 & 0 & 0 & 0 & 0 \\ 0 & 0 & 0 & 0.0000 & 0 & 0 \\ 0 & 0 & 0 & 0 & 0.0000 & 0 \\ 0 & 0 & 0 & 0 & 0 & 0.0000 \end{bmatrix}$$

Then we need to translate USBL matrix to gravity center of the entire body using the translational vector [0.44; 0; -0.14]. Therefore the translated USBL added mass matrix is shown below:

$$M_{usbl}^{CG} = \begin{bmatrix} 0.0605 & 0 & 0 & 0 & -0.0085 & 0 \\ 0 & 0.0320 & 0 & 0.0045 & 0 & 0.0141 \\ 0 & 0 & 0 & 0 & 0 & 0 \\ 0 & 0.0045 & 0 & 0.0006 & 0 & 0.0020 \\ -0.0085 & 0 & 0 & 0 & 0.0012 & 0 \\ 0 & 0.0141 & 0 & 0.0020 & 0 & 0.0062 \end{bmatrix}$$

The values of the USBL matrix are too small to significantly affect the overall added mass matrix. Thus, the USBL object, along with objects contributing even less than the USBL, can be neglected. After computing the added mass matrices of all Sparus elements and performing their final summation, the resulting added mass matrix is shown below:

$$M_{full}^{CG} = \begin{bmatrix} 2.0988 & 0 & 0 & 0 & -0.0181 & 0 \\ 0 & 58.5172 & 0 & 0.2676 & 0 & 10.4036 \\ 0 & 0 & 62.5830 & 0 & -7.8239 & 0 \\ 0 & 0.2676 & 0 & 0.2243 & 0 & -0.1172 \\ -0.0181 & 0 & -7.8239 & 0 & 16.9890 & 0 \\ 0 & 10.4036 & 0 & -0.1172 & 0 & 15.3148 \end{bmatrix}$$

It is also possible to neglect terms which are less than 0.1 because of their small impact on the body. Therefore the final main body added mass matrix is shown below:

$$M_{finalfull}^{CG} = \begin{bmatrix} 2.10 & 0 & 0 & 0 & 0 & 0 \\ 0 & 58.52 & 0 & 0.27 & 0 & 10.40 \\ 0 & 0 & 62.58 & 0 & -7.82 & 0 \\ 0 & 0.27 & 0 & 0.22 & 0 & -0.12 \\ 0 & 0 & -7.82 & 0 & 16.99 & 0 \\ 0 & 10.40 & 0 & -0.12 & 0 & 15.31 \end{bmatrix}$$

Work to do 4:

Compare this matrix at CG and CB. Is it important to take into account the distance between the two points ?

The added mass matrix after translation to the buoyancy center, using the translation vector [0; 0; -0.02] is shown below:

$$M_{full}^{CB} = \begin{bmatrix} 2.10 & 0 & 0 & 0 & 0 & 0 \\ 0 & 58.52 & 0 & 0.31 & 0 & 10.40 \\ 0 & 0 & 62.58 & 0 & -7.82 & 0 \\ 0 & 0.23 & 0 & 0.22 & 0 & -0.12 \\ 0 & 0 & -7.82 & 0 & 16.99 & 0 \\ 0 & 10.40 & 0 & -0.12 & 0 & 15.31 \end{bmatrix}$$

In this case, the translation for 0.02 m did not significantly impact the overall added mass matrix. However, the coupled coefficients were affected. For m_{24} and m_{42} , this effect is attributed to the presence of the antenna. All other values remain unaffected due to the XZ symmetry of Sparus.

Work to do 5:

Compare the values of the main solid with the others and conclude.

1. Main Body vs Antenna:

- The main body has significantly higher added mass values compared to the antenna. This is expected due to its larger dimensions (1.6 m vs 0.256 m length).
- Added mass in sway (m_{22}) and heave (m_{33}) for the main body are 57.33, while for the antenna these values are much smaller ($m_{22} = 1.19$, $m_{33} = 0$).
- The difference highlights the larger hydrodynamic influence of the main body in these directions, the bigger water displacement.

2. Main Body vs Thrusters:

- The main body also has significantly higher added mass values compared to the thrusters due to its larger volume and cross-sectional area.
- For example, m_{33} (heave) for the main body is 57.33, whereas for a single thruster it is only 2.63.
- Rotational coefficients (e.g., m_{55}) also show a clear difference: 15.05 for the main body vs 0.96 for the thrusters.

3. Main Body vs USBL:

- The dimensions of the USBL are much smaller than the main body, and its added mass values are negligible compared to the main body.
- For example, even m_{11} (surge) for the USBL is 0.06, whereas for the main body it is 1.60.
- Consequently, the USBL can be neglected in the global added mass matrix due to its minimal hydrodynamic influence.

Work to do 6:

Compare the added and real mass matrix and conclude.

- The added mass matrix accounts for the hydrodynamic influence of water on the vehicle's motion. It adds significant contributions in rotational and coupled terms.

- For the main body, the real mass matrix is diagonal with constant mass $m = 52\text{ kg}$. In contrast, the diagonal terms of the added mass matrix are not constants due to different water affection due to Sparus' geometry.
- The influence of water displacement increases the vehicle's inertia, especially in sway (m_{22}) and heave (m_{33}), where the added mass values are significant.
- Translational and rotational coupled terms (m_{ij} , where $i \neq j$) in the added mass matrix are important for the dynamic modeling and give more precise information.
- This comparison highlights that the added mass matrix cannot be ignored in underwater vehicle dynamics as it shows the hydrodynamic effects that the real mass matrix does not.

Work to do 7:

Estimate all drag matrices.

Only the main body, thrusters, and antenna are considered to estimate the drag matrices of different parts. The drag matrices for the USBL are so small that they have been ignored.

The drag matrix is initially expressed in the component's buoyancy centre and then transferred to the gravity centre of the AUV. The simple estimation of shapes has been made for different parts.

Sections	3DDragShape	2DDragShape
Main body	Ellipsoid($\frac{L}{D} = 7.04$)	Circular rod(Cylinder)
Antenna	Rectangular Plate	
Thrusters	Finite Cylinder, horizontal, $A = \frac{\pi D^2}{4}$	Rectangular Plate, $A = LD$

Table 2: Drag shapes for different sections

- Main Body: The main body's 3D shape is considered to be Ellipsoid with $\frac{L}{D} = 7.04$, and the 2D shape is a circular rod (cylinder).

$$C_{DL} = 0.26, C_{DT} = 0.105, L_0 = 0.094, L_1 = 1.28, L_2 = 0.23, L = 1.6, R = 0.1126, \rho = 10^3$$

The flow is considered to be turbulent

$$D = \begin{bmatrix} K_{11} & 0 & 0 & 0 & 0 & 0 \\ 0 & K_{22} & 0 & 0 & 0 & 0 \\ 0 & 0 & K_{33} & 0 & 0 & 0 \\ 0 & 0 & 0 & K_{44} & 0 & 0 \\ 0 & 0 & 0 & 0 & K_{55} & 0 \\ 0 & 0 & 0 & 0 & 0 & K_{66} \end{bmatrix}$$

$$D_{MainBody} = \begin{bmatrix} 2.1285 & 0 & 0 & 0 & 0 & 0 \\ 0 & 54.528 & 0 & 0 & 0 & 0 \\ 0 & 0 & 54.528 & 0 & 0 & 0 \\ 0 & 0 & 0 & 0 & 0 & 0 \\ 0 & 0 & 0 & 0 & 6.9796 & 0 \\ 0 & 0 & 0 & 0 & 0 & 6.9796 \end{bmatrix}$$

- Antenna: Considering the antenna as a rectangular plate, $A = LD$

$$C_{D_{22}} = C_{D_S} = 1.01 + 0.02\left(\frac{L}{D} + \frac{D}{L}\right) = 1.174,$$

Here, $L = 0.256$, $D = 0.076$ Again,

$$C_{D_{11}} = C_{D_B} = 1.01 + 0.02\left(\frac{L}{D} + \frac{D}{L}\right) = 1,302,$$

Here, $L = 0.256$, $D = 0.0256$

$$D_{Antenna} = \begin{bmatrix} 4.266 & 0 & 0 & 0 & 0 & 0 \\ 0 & 11.421 & 0 & 0 & 0 & 0 \\ 0 & 0 & 0 & 0 & 0 & 0 \\ 0 & 0 & 0 & 0 & 0 & 0 \\ 0 & 0 & 0 & 0 & 0.002237 & 0 \\ 0 & 0 & 0 & 0 & 0 & 0.00599 \end{bmatrix}$$

- Thrusters: Considering thrusters as a 3D finite cylinder in x, calculate

$$K_{11} = 5.0895, \frac{L}{D} = \frac{0.2405}{0.12} = 2.009, C_D = 0.9, S_x = 0.01131$$

Considering it rectangular in z:

$$K_{22} = 0$$

$$K_{33} = 36.075, C_D = 2.5, L = 0.12, D = 0.2405$$

$$K_{44} = 0$$

$$K_{55} = 0.00195$$

$$K_{66} = 0$$

$$D_{Thrusters} = \begin{bmatrix} 5.0895 & 0 & 0 & 0 & 0 & 0 \\ 0 & 0 & 0 & 0 & 0 & 0 \\ 0 & 0 & 36.075 & 0 & 0 & 0 \\ 0 & 0 & 0 & 0 & 0 & 0 \\ 0 & 0 & 0 & 0 & 0.00195 & 0 \\ 0 & 0 & 0 & 0 & 0 & 0 \end{bmatrix}$$

Incorporating negative values into the drag matrix is crucial for accurate computations. The drag force acts as a damping force, opposing the movement of the Sparus, and thus plays a significant role in the system's overall dynamics. Negative values in the drag matrices are necessary to represent the opposing direction of the force, which ensures the correct modelling of the vehicle's resistance to motion. Additionally, failing to account for these negative values could lead to incorrect predictions of the Sparus' behaviour, potentially affecting control strategies and performance assessments in real-world applications.

Work to do 8:

Complete the simulator with some simple experiments to validate it.

The Sparus AUV is equipped with three thrusters: one vertical and two horizontal. This configuration enables control over three Degrees of Freedom (DOF): Surge, Heave, and Yaw.

To validate the dynamic model, various test cases are employed to observe their effects on the simulated AUV.

In the simulation, thruster forces are modified to analyze their impact on the position, velocity, and acceleration of the AUV over a time frame of 100 seconds. These adjustments provide insights into the dynamic response and maneuverability of the vehicle under different control inputs.

Experiment 1: Surge motion along X axis (Figure 2)

Surge motion should demonstrate stability during execution. By activating the right and left thrusters at 20% power along the positive x-axis direction, the craft exhibited forward movement. Analysis of the resulting motion plots shows that the surge velocity initially peaked and then maintained a steady constant value.

However, the lack of control over the craft's angular velocity in the y-direction (pitch) resulted in some oscillations. This instability underscores the need for mechanisms to manage angular dynamics effectively.

As the Sparus accelerates, it attempts to return to its mean position, causing the surge acceleration to eventually stabilize at zero. Despite this, the absence of control over angular acceleration in the y-direction contributes to significant oscillations in the vehicle's body, attributed to angular pitch acceleration.

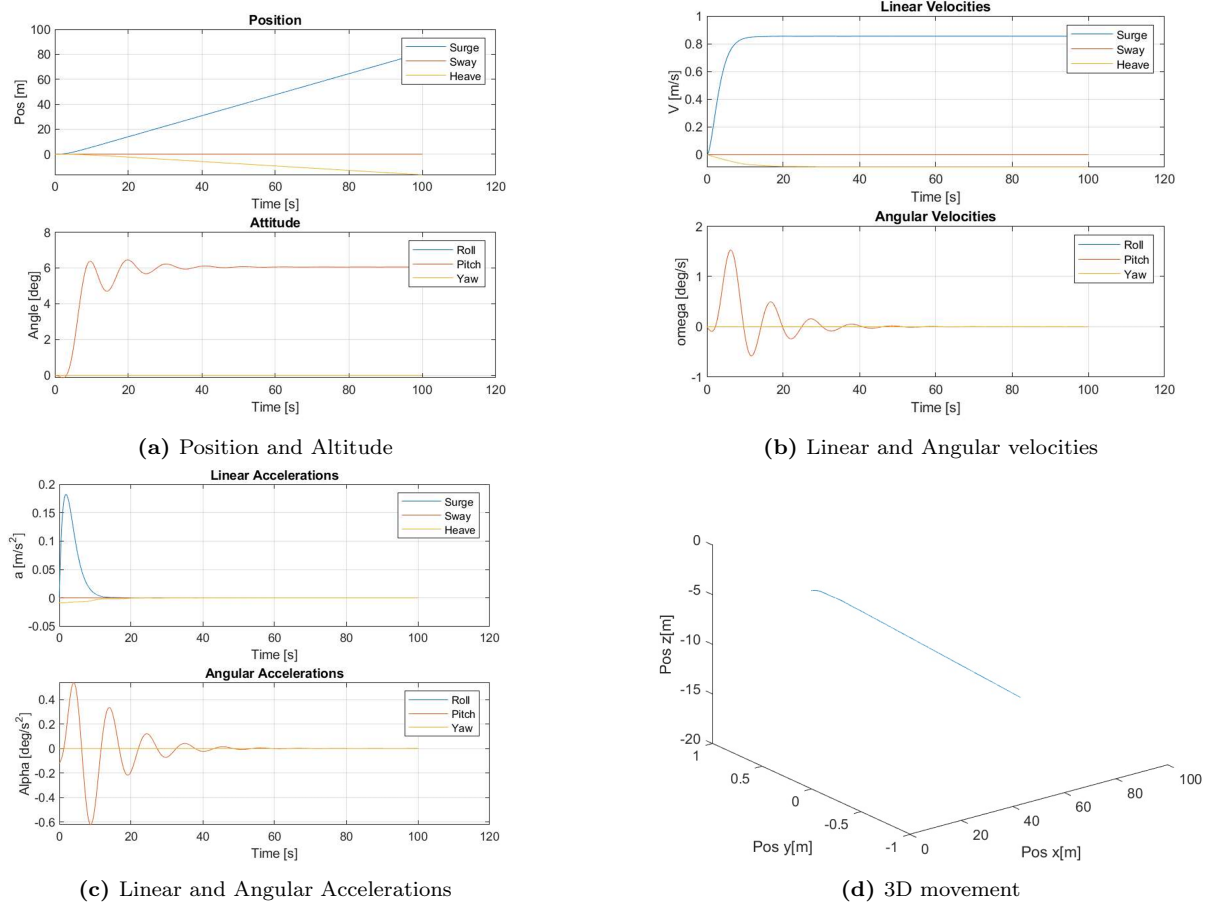


Figure 2: Simulation Result for Experiment 1 (Surge motion along X axis)

Experiment 2: Heave motion along Z axis (Figure 3)

Heave motion should ideally show stability during execution. By activating the vertical thruster at 20% power along the positive z-axis direction, the craft demonstrated a controlled descent into the water. From the velocity graph, it is evident that the AUV achieves its maximum

velocity in the heave direction and subsequently sustains a constant velocity.

This heave motion directly impacts the angular velocity of the craft. Due to the lack of control over the robot's pitch, oscillations and disturbances in the angular velocity persist. These disturbances highlight the coupling effects between translational and rotational motions, particularly in cases when there is no angular stabilization mechanisms.

The inability to manage pitch effectively during heave motion could result in operational inefficiencies, especially in tasks requiring precise vertical maneuvers. Incorporating advanced control algorithms or additional actuation systems to stabilize angular dynamics may significantly improve the AUV's performance and reliability in underwater missions. Such enhancements are crucial for ensuring stable and predictable behavior during complex underwater operations.

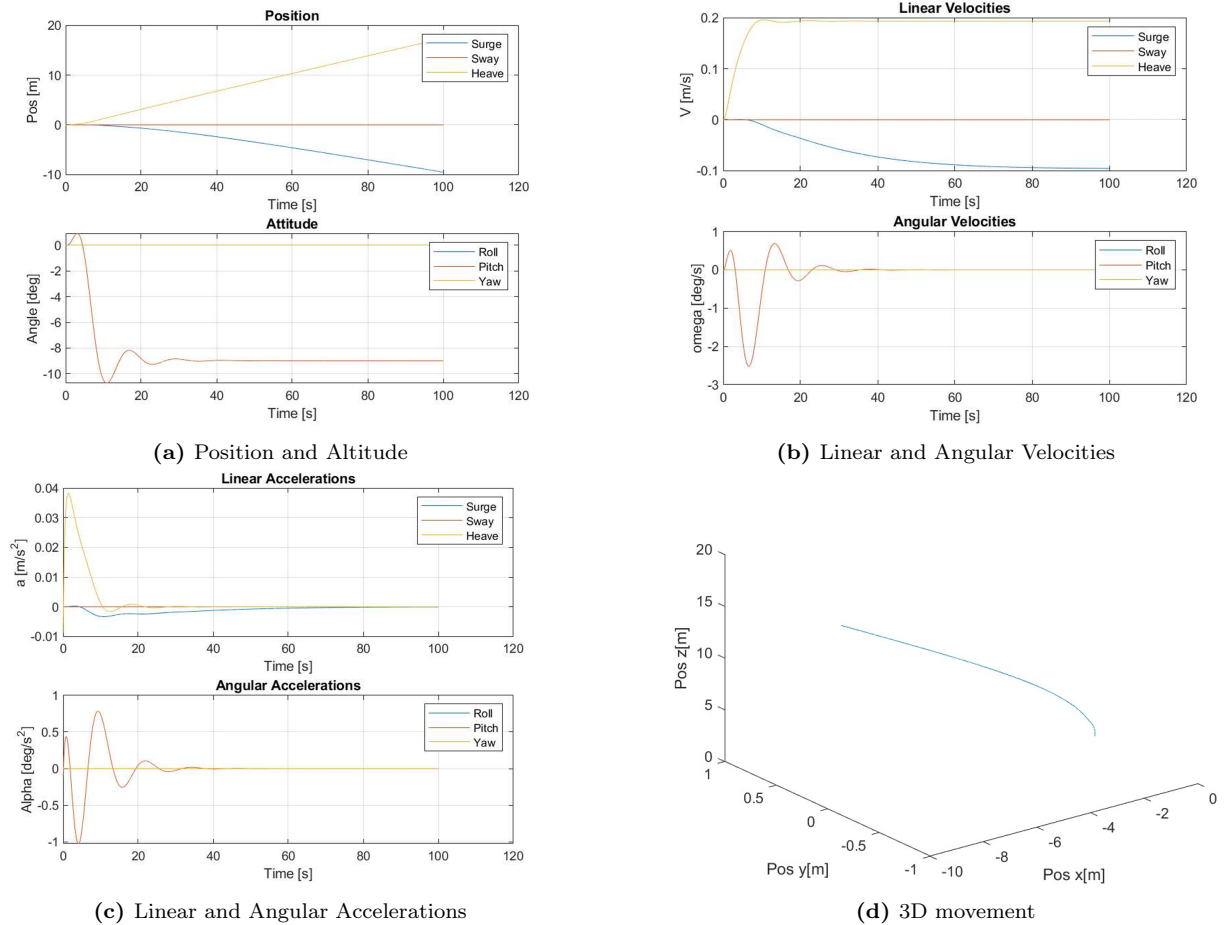


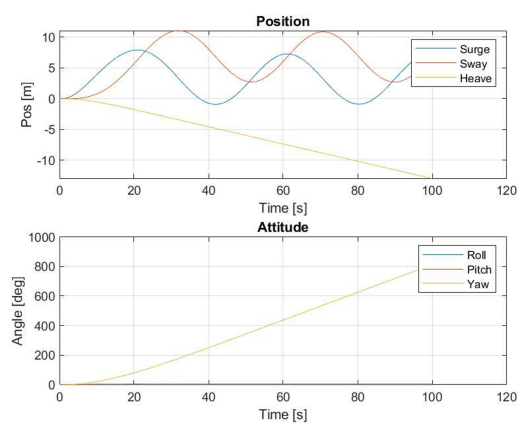
Figure 3: Simulation Result for Experiment 2 (Heave motion along Z axis)

Experiment 3: Yaw motion around Z axis (Figure 4)

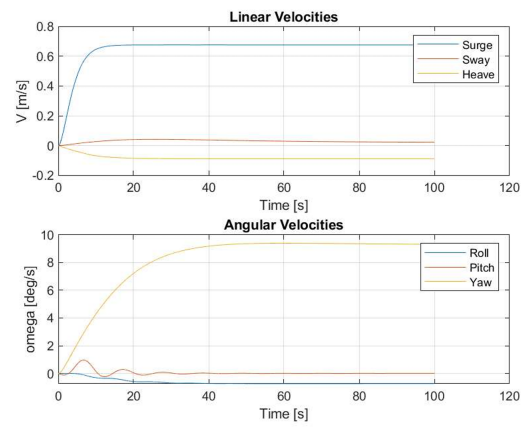
Yaw motion should ideally show stability during execution. By activating the right thruster at 10% power in the positive x-axis direction and the left thruster at 15% power, the craft initiates a left turn.

Analysis of the resulting plots shows that the yaw velocity reaches a specific value and then maintains a constant angular velocity.

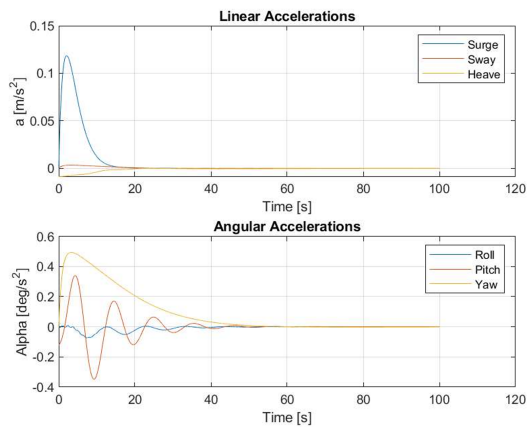
However, when adjusting the periodic depth during pure yaw motion, caution is required due to the craft's buoyancy. The buoyant forces acting on the AUV can influence its vertical position, leading to unintended changes in depth while executing Yaw movements. These depth variations can disrupt the precision of yaw control and may cause instability if not properly compensated for.



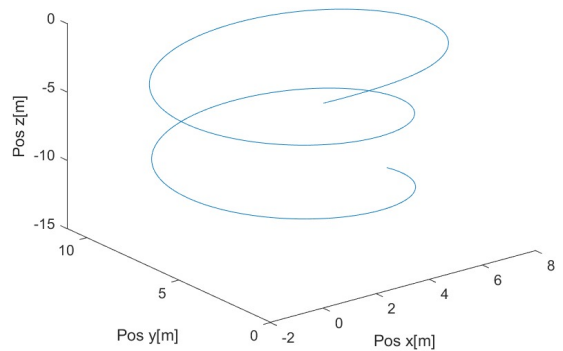
(a) Position and Altitude



(b) Linear and Angular Velocities



(c) Linear and Angular Accelerations



(d) 3D movement

Figure 4: Simulation Result for Experiment 3 (Yaw motion around z axis)

Work to do 9:

Find some simulations to highlight the impact of the different coefficients in the global mass matrix. (Impose linear accelerations)

To assess the impact of various coefficients in the global mass matrix, certain shapes considered during the analysis can be assumed to have negligible effects. By excluding these shapes from the model, the resulting changes in the global mass matrix and their influence on the simulation can be evaluated. This approach enables the examination of how the omission of specific components affects the overall system behavior, providing a clearer understanding of the relevance of each shape in the mass matrix. The observed variations in the simulation outcomes highlight the importance of the neglected shapes and the accuracy of the reduced model.

Let's see the plots considering the antenna and the thrusters first.

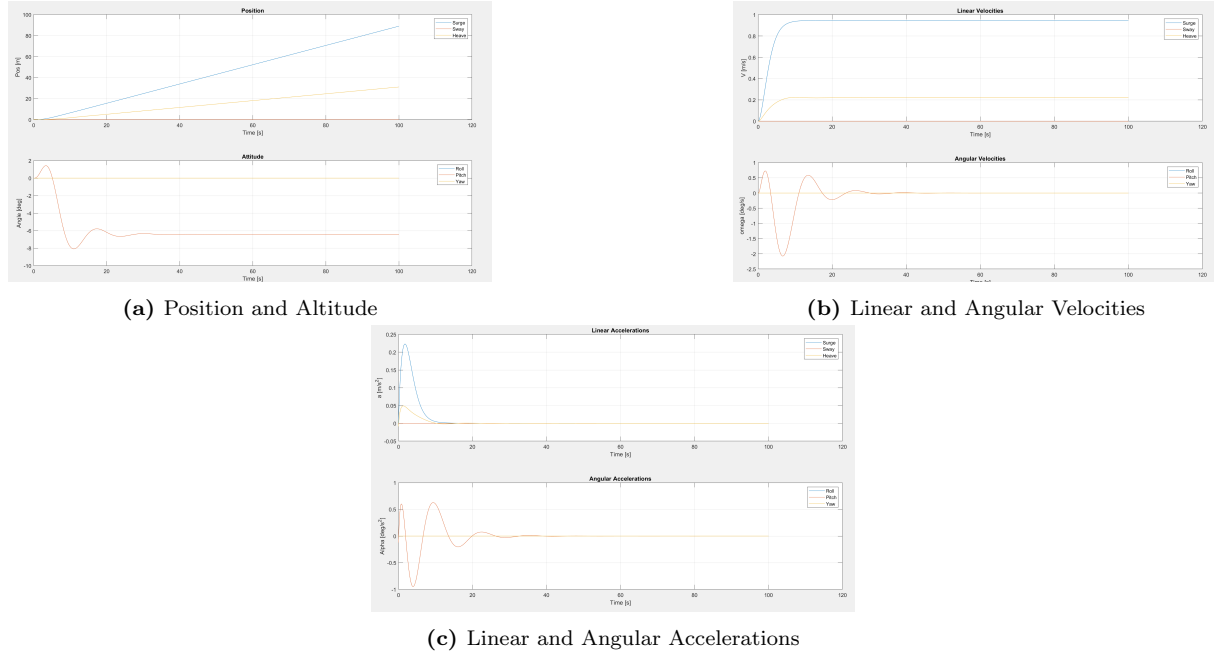


Figure 5: Simulation Results Considering the added mass of Antenna and Thrusters

Antenna: It was observed that the antenna estimation has minimal effect on the estimation of the forces and moments that influence the linear and angular accelerations affecting the Sparus. Therefore, it could have been neglected in the analysis without significantly impacting the results. Figure 5 shows the Sparus' motion considering the antenna and both thrusters, when Figure 6 shows the motion with neglected antenna.

Thrusters: It was observed that the added mass estimation of the thrusters has a negligible effect on the estimation of the forces and moments influencing the linear and angular accelerations that affect the Sparus. Therefore, the added mass of the thrusters could have been neglected in the analysis without significantly impacting the overall results. This finding suggests that the influence of the thruster's added mass on the vehicle's dynamics is minimal under the given conditions, allowing for simplification in the modeling process. Figure 7 shows the motion with neglected antenna.

These observations highlight the robustness of the model, showing that certain details, such as the added mass of the thrusters or antenna, may be omitted without compromising the integrity of the analysis. This simplification could lead to more efficient computations while maintaining an acceptable level of precision in the results.

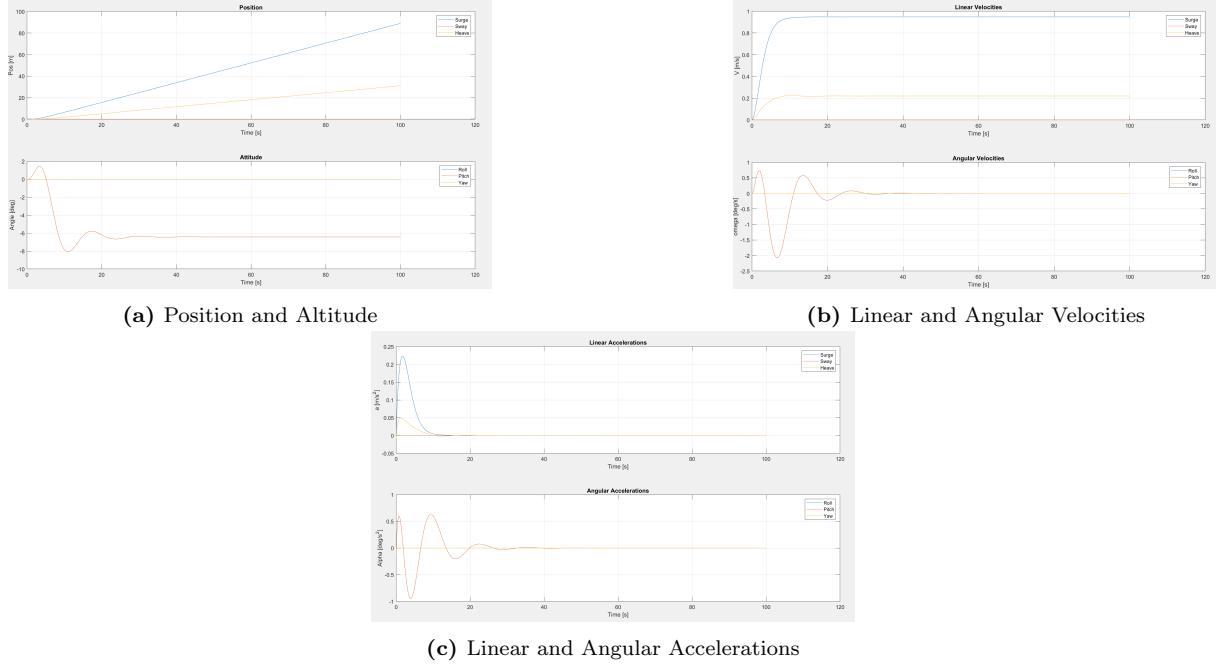


Figure 6: Simulation Results Without Considering the added mass of Antenna

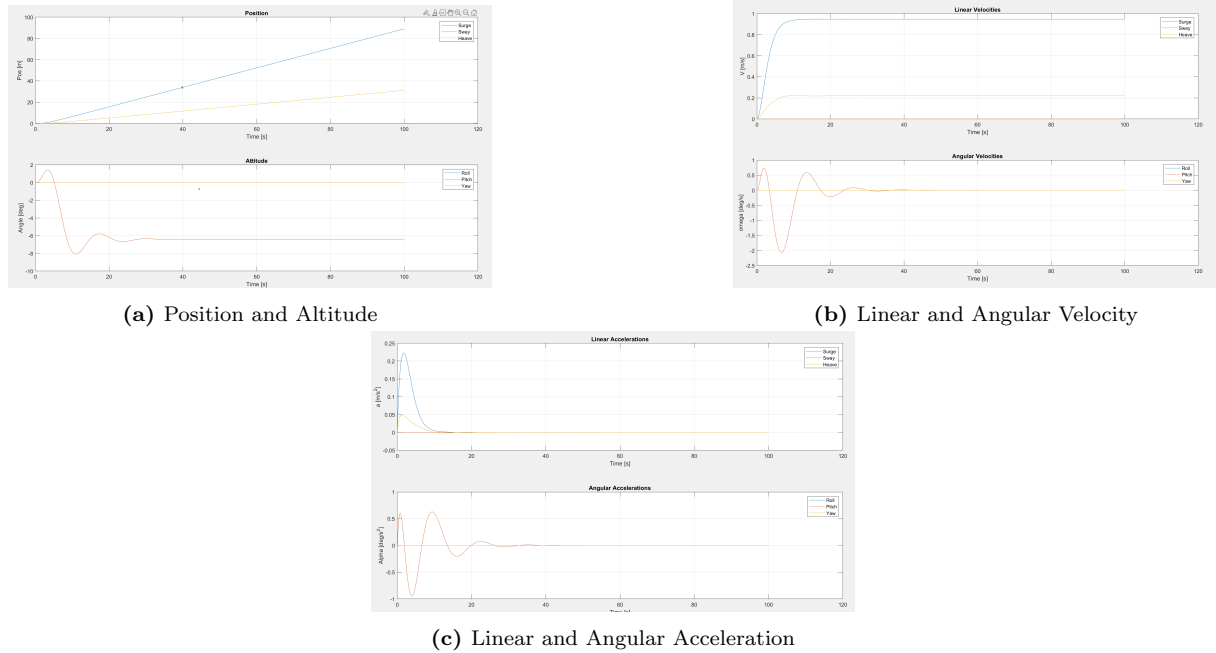


Figure 7: Simulation Results Without Considering the added mass of Thruster

Work to do 10:

Find some simulations to highlight the impact of the drag forces of the different bodies (Impose constant linear speed)

To examine the impact of drag, which is responsible for the damping of the Sparus, the drag coefficients were set to zero to observe the vehicle's response. In the simulation, all thrusters were set to 25% power, and an initial velocity of 10 m/s was applied along the x-direction, with the vehicle positioned at the origin. The simulation ran for 100 seconds to analyze the resulting motion and evaluate the influence of drag on the vehicle's dynamics.

By removing the drag forces, the focus is on observing how the Sparus responds without the damping effects, providing a clearer understanding of the vehicle's behavior in the absence of drag. This setup enables an analysis of the vehicle's performance under ideal conditions and highlights the crucial role of drag in practical underwater applications.

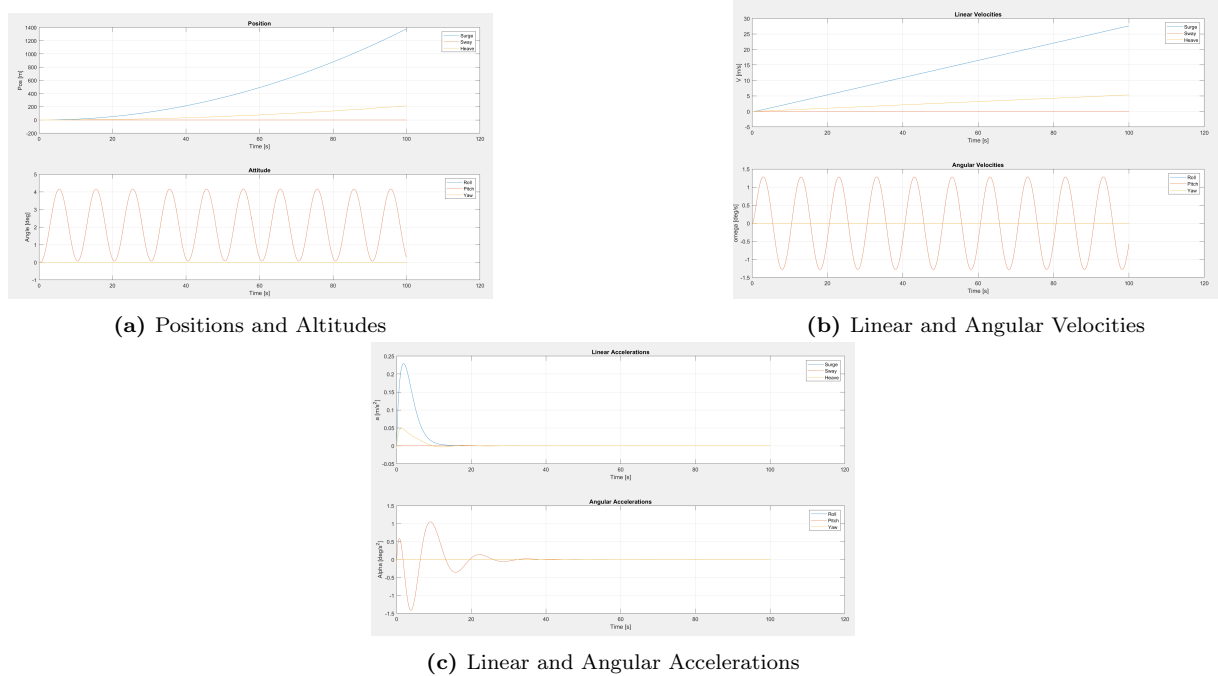


Figure 8: Simulation Results Without Considering Any Drag Forces

When drag coefficients are considered, if an initial constant linear speed is provided, it was observed that the speed decreases exponentially due to damping forces and stabilizes once it balances out the drag (reaches equilibrium). This behavior is typical in systems experiencing damping, where the velocity gradually reduces and becomes constant as the energy dissipates through friction and drag forces.

In a viscous fluid, the presence of damping forces leads to a non-conservative system in terms of energy, often referred to as interference drag. This type of drag arises from vortex sheet shedding at sharp edges, which generates additional damping forces on the body. These forces oppose the motion of the vehicle, causing it to lose energy in the form of heat and turbulence, ultimately reducing its speed.

If the drag coefficient is removed from a body submerged in the fluid, the system becomes unstable, and the vehicle experiences oscillations. Without the drag forces to dampen the motion, the vehicle's movement becomes uncontrollable, leading to sustained oscillations that may cause instability. This highlights the essential role of drag in maintaining stability and

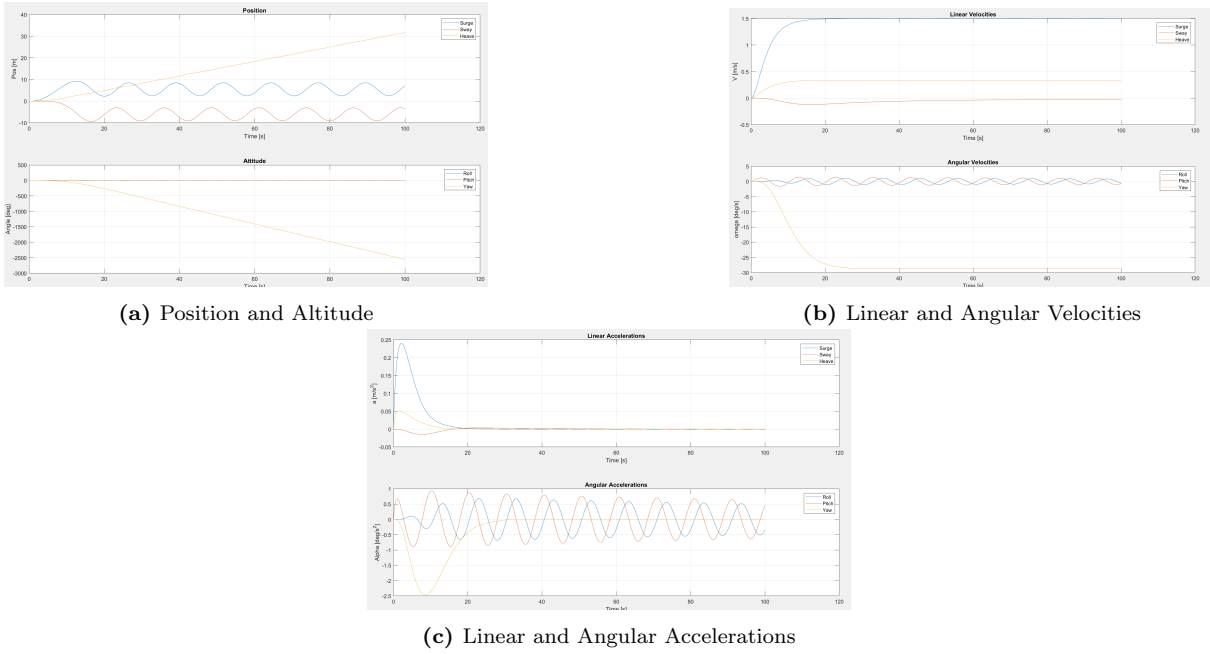


Figure 9: Simulation Results Without Considering Drag Forces of Thrusters and Antenna

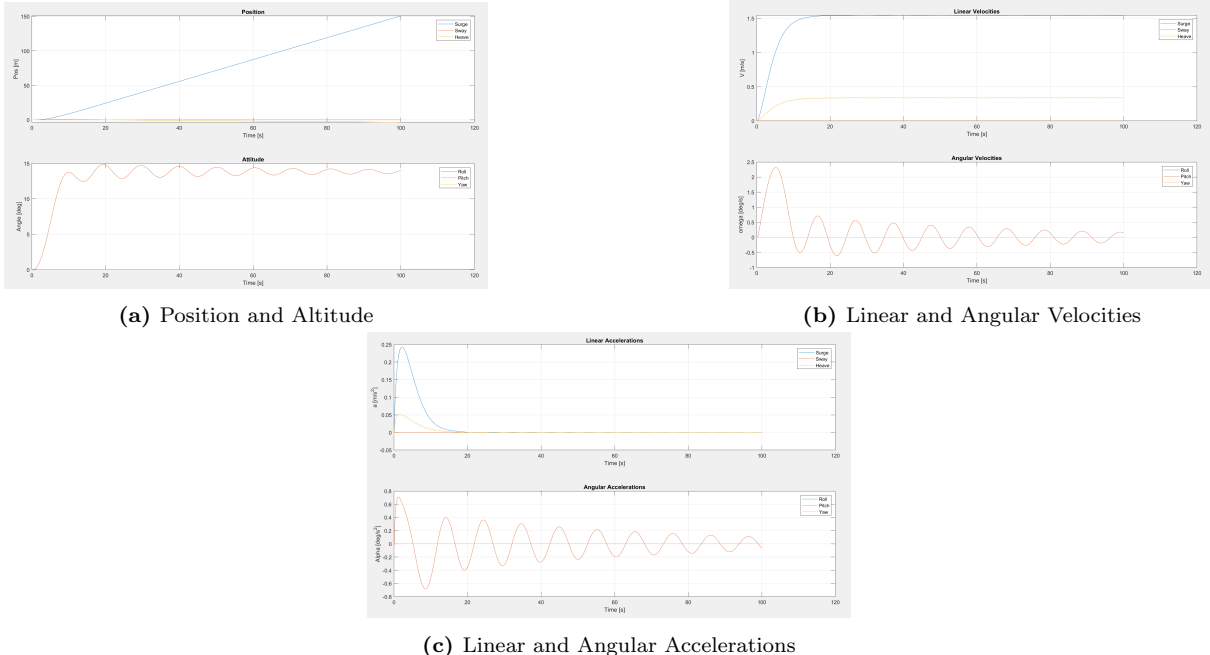


Figure 10: Simulation Results Without Considering the Drag Forces of Thrusters

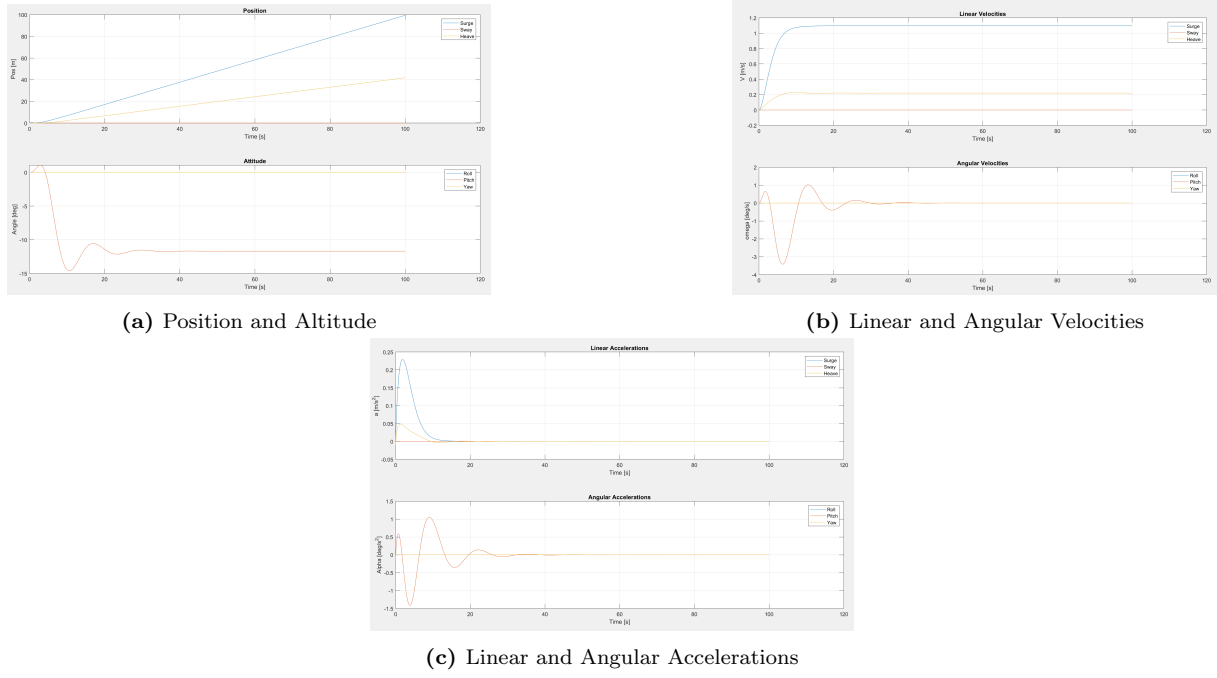


Figure 11: Simulation Results Without Considering the Drag Forces of the Antenna

control in underwater vehicles, as its removal would compromise the ability to regulate motion and manage the vehicle's trajectory.